ACS OMEGA

http://pubs.acs.org/journal/acsodf

Article

Impact of a Diverse Combination of Metal Oxide Gas Sensors on Machine Learning-Based Gas Recognition in Mixed Gases

Garam Bae, Minji Kim, Wooseok Song,* Sung Myung, Sun Sook Lee, and Ki-Seok An*

Cite This: *ACS Omega* 2021, 6, 23155−23162

Read Online

ACCESS | Metrics & More | Article Recommendations | Supporting Information

ABSTRACT: A challenge for chemiresistive-type gas sensors distinguishing mixture gases is that for highly accurate recognition, massive data processing acquired from various types of sensor configurations must be considered. The impact of data processing is indeed ineffective and time-consuming. Herein, we systemically investigate the effect of the selectivity for a target gas on the prediction accuracy of gas concentration *via* machine learning based on a support vector machine model. The selectivity factor $S(X)$ of a gas sensor for a target gas "X" is introduced to reveal the correlation between the prediction accuracy and selectivity of gas sensors. The presented work suggests that (i) the strong correlation between the selectivity factor and prediction accuracy has a proportional relationship, (ii) the enhancement of the prediction accuracy of an elemental sensor with a low sensitivity factor can be attained by a complementary combination of the other sensor with a high selectivity factor, and (iii) it can also be boosted by combining the sensor having even a low selectivity factor.

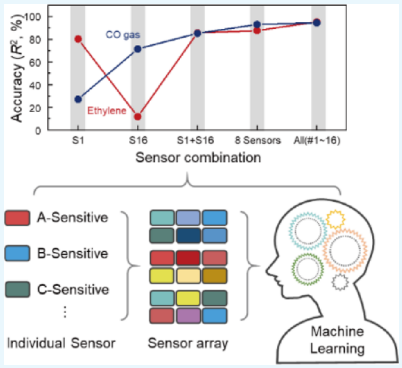

INTRODUCTION

A central hurdle in the recent research fields for chemiresistive-type gas sensors is to gain selectivity for a target analyte, which greatly impedes their further development.[1−7] In typical chemiresistive-type gas sensors, the gas response of target analytes can be extracted from the variation in measurable electrical signals stimulated by charge interactions between the gas molecules and the semiconductor surface. Recently, considerable interest has focused on boosting the response of specific gases to gain gas selectivity. Two representative strategies are available to enhance the gas selectivity of chemiresistive-type gas sensors. First, the diversification of the device is currently being pursued beyond simple resistor-type devices. It has been demonstrated that gas sensors based on p-n junctions are able to realize high selectivity through the gas adsorption-dependent modulation of a space charge region between the p-n junctions, which is attributable to the alteration in carrier concentration before and after the surface adsorption of target gases.[8−10] Similarly, a barristor-type gas sensor secured the selectivity by maximizing the response *via* modulation of the Schottky barrier height between the heterojunctions associated with gas adsorption-stimulated variation in the work function.[11,12] Second, surface modification and functionalization of sensing materials have been adopted concentrically to engineer the gas adsorption energy at the surface of the sensing materials. To achieve gas selectivity, metal−organic frameworks have been utilized on the surface of sensing materials for gas filtering *via* a molecular sieving effect.[13−15] A combination of a polar siloxane polymer layer and metal oxide thin films has also been implemented to discriminate between polar and nonpolar gases for volatile organic compound gases.[16,17] In addition, considerable interest has focused on the complementary hybridization of metal oxides and catalysts to reduce the activation energy for the charge interaction of adsorbed specific analytes with the sensing materials.[18,19]

Based on these results, it can be deduced that central research to achieve the gas selectivity of chemiresistive-type gas sensors has been constrained to boost the response of a specific gas among diverse gases, which is distinctly accompanied with limited research on sensing materials and device architecture. In general, the gas response relies on the combination of target gas selectivity and its concentration, which can be defined as follows

$$\text{response}(X) = \alpha \cdot S(X) \cdot C(X) \quad (1)$$

where α is an environmental factor containing the working pressure, the volume of the container, the surface-to-volume area for the sensing material, the temperature, the humidity, etc. $S(X)$ is the selectivity factor for the target gas X, and $C(X)$ is its concentration. The selectivity factor can be determined by the correlation between the absorption energy and the activation energy for the charge interaction with gas molecules. In general, a gas sensor with high selectivity for A gas is

Received: May 25, 2021
Accepted: August 16, 2021
Published: September 3, 2021

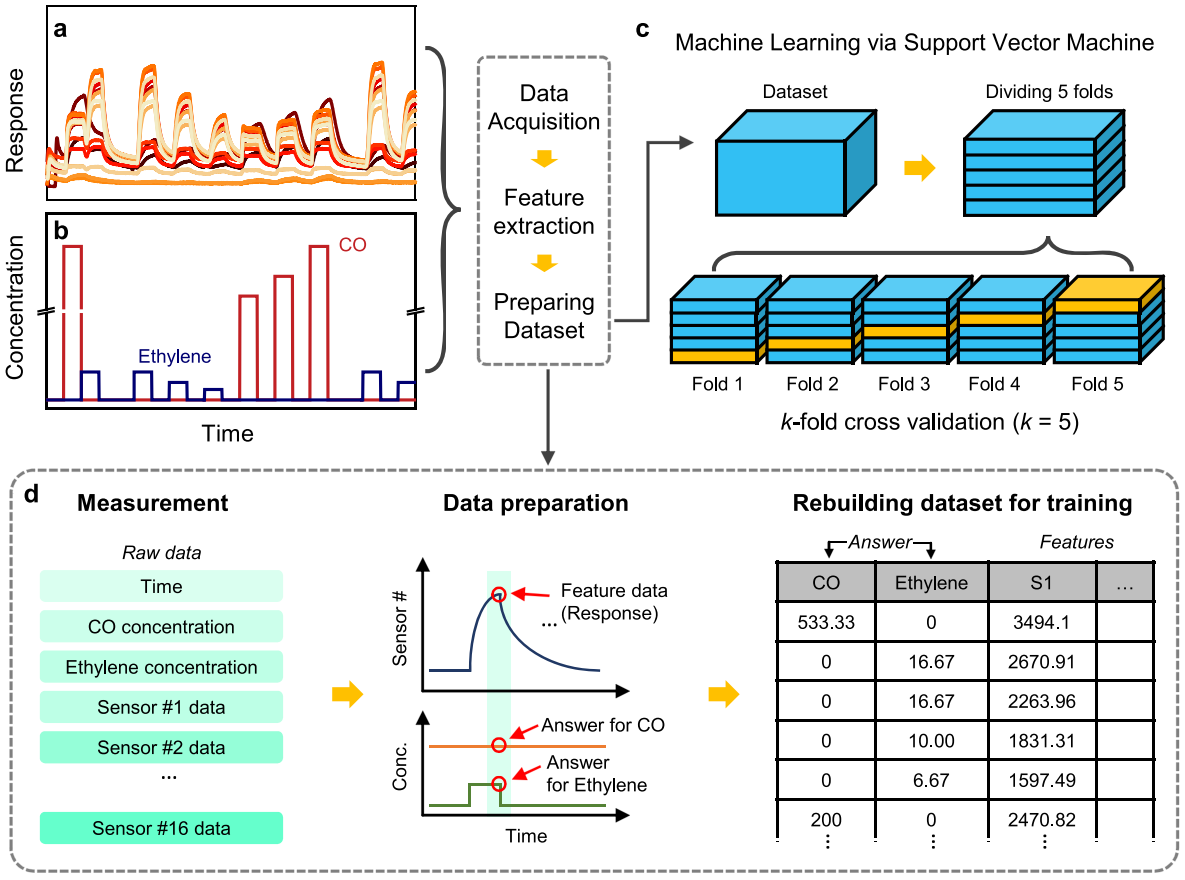

Figure 1. (a) Dynamic response curves acquired from an array of 16 commercial gas sensors (b) under exposure to mixture gases with diverse concentration. (c) Schematic illustration of the machine learning (ML) process with a support vector machine (SVM) model based on the *k*-fold (k = 5) cross-validation protocol. (d) Schematic diagram of data preparation for ML.

relevant to a higher $S(A)$ value compared with $S(B)$, $S(C)$, ..., and $S(X)$ values corresponding to the B, C, ..., and X gases ($S(A) \gg S(B)$, $S(C)$, ... and $S(X)$), respectively. In this regard, it is noted that two cases associated with a higher $S(A)$ value combined with a lower $C(A)$ and a lower $S(A)$ value with higher $C(A)$ are indistinguishable. These relationships can be summarized as follows

$$S(A) \gg S(B) \text{ and } C(A) \ll C(B) \rightarrow \text{response(A)} \approx \text{response(B)} \quad (2)$$

To overcome this unattainable hurdle, an alternative strategy involving machine learning (ML) based on statistical data processing has recently attracted tremendous interest, which corroborates new insights into the capability of identifying a target gas in undefined gaseous mixtures using a simple analytical comparison of gas responses.[20,21] However, a vast amount of data is indispensable for ML with guaranteed accuracy, which encounters a limitation that an inefficient process for additional distinct feature extraction is needed.[22,23] To address this issue, for simplification of processes, we accordingly investigated the effect of the selectivity of an individual gas sensor for the target gas on the prediction accuracy of gas concentration *via* machine learning based on a support vector machine (SVM) model. The SVM is connected to an algorithm for building a predictive machine learning model, which strongly relies on statistical learning theory based on the idea of finding the best separating hyperplane of two point sets in the sample space in terms of classification error and separation margin. There are several ML-assisted gas recognition models using artificial neural networks (ANN), principal component analysis (PCA), and K-nearest neighbors (KNN). However, those approaches are still limited on the practical application due to the strong dependency on the initial selection of weights and thresholds, relatively poor accuracy, and the memory issue on storing the massive data.[24−26] Since the SVM can effectively resolve the above-mentioned problems and it is a simple and effective technique for quantitatively analyzing gas mixtures as this can address the cross sensitivity problem of gas sensor arrays, it has emerged as a promising candidate for general classification and regression in a wide range of research fields, such as pattern recognition, material design, and the prediction of material's properties.[27−29] The response gained from an array of 16 gas sensors for ethylene and CO mixture gases, a representative and easily accessible feature, was allocated as the feature data for ML. Electrochemical conversion from carbon monoxide (CO) to ethylene, which is one of the important building blocks for the chemical industry and usually produced by steam cracking of naphtha feedstocks at 800−900 °C, has been actively studied and considered as an energy-efficient electrochemical reduction process.[30−32] Therefore, the implementation of a selective detection device should be done for an accurate quantitative analysis of each individual gas from CO and ethylene mixture gases. To validate the correlation between the selectivity and prediction accuracy, the selectivity factor, $S(X)$, was deduced *via* a systematic study of the gas response with altering multigas concentrations. Then, optimized conditions associ-

https://doi.org/10.1021/acsomega.1c02721
ACS Omega 2021, 6, 23155−23162

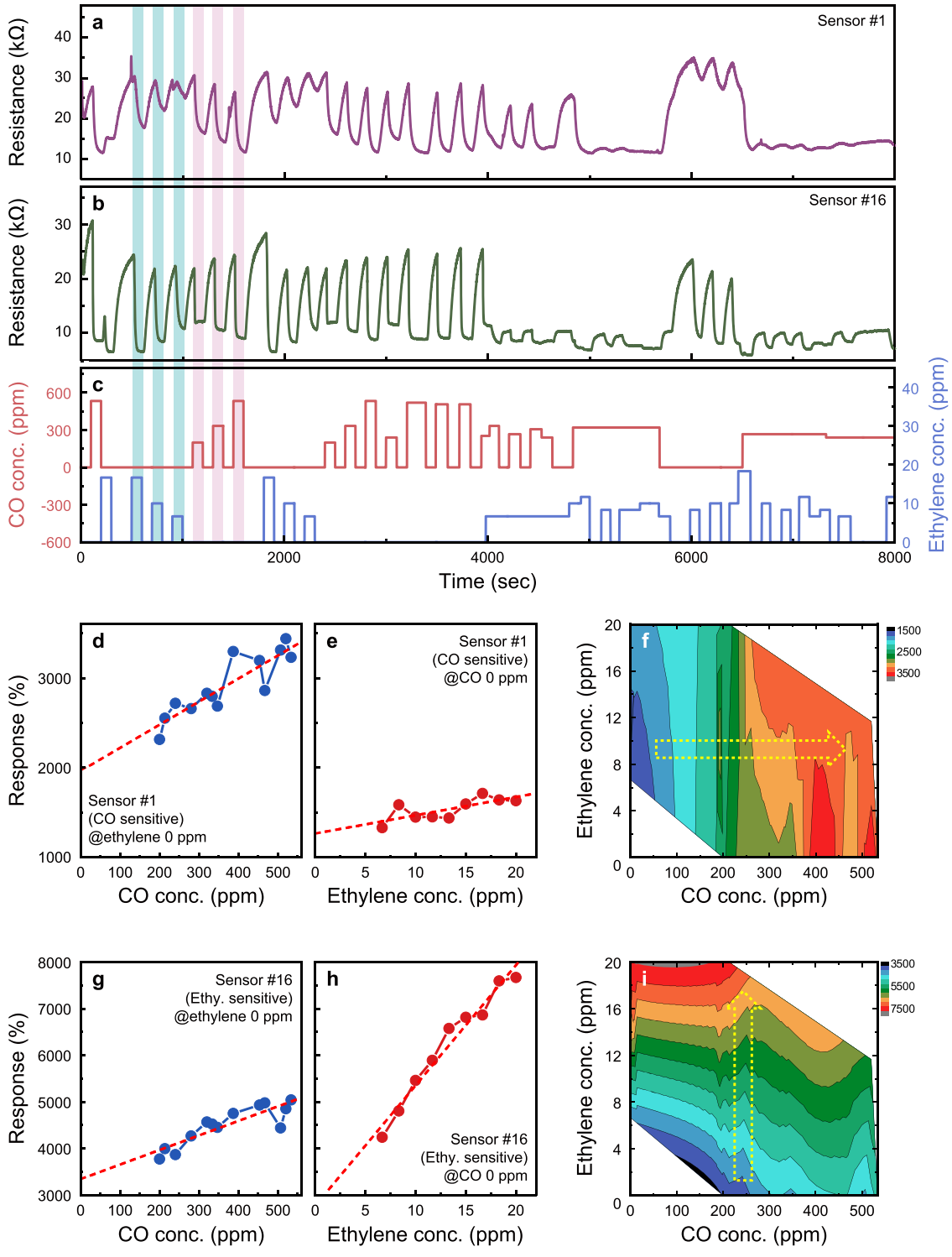

Figure 2. Dynamic gas response curves of (a) sensor #1 and (b) sensor #16 for CO and ethylene gases with diverse concentration and (c) gas concentration profile (red (blue) shaded regions: CO (ethylene) without ethylene (CO)). Correlations between gas response values gained from sensor #1 for (d) CO and (e) ethylene and their concentration. (f) Contour plot for gas response of sensor #1 for both CO and ethylene concentrations. Plot of gas response values gained from sensor #16 for (g) CO and (h) ethylene as a function of their concentration. (i) Contour plot for gas response of sensor #16 for both CO and ethylene concentrations.

ated with a combination of individual sensors were derived to improve the prediction accuracy of ML for gas concentrations.

RESULTS AND DISCUSSION

To verify the validity of the proposed strategy, an open sensor array dataset collected from the University of California Irvine (UCI) was used, which contains the dynamic gas responses gained from arrays of 16 commercial sensors (TGS2600, TGS2602, TGS2610, and TGS2620; four units of each type) under ethylene and CO mixtures in air with diverse concentrations.[30] The operating temperature can be adjusted by 5 V of applied voltage, which was integrated with a chip

https://doi.org/10.1021/acsomega.1c02721
ACS Omega 2021, 6, 23155−23162

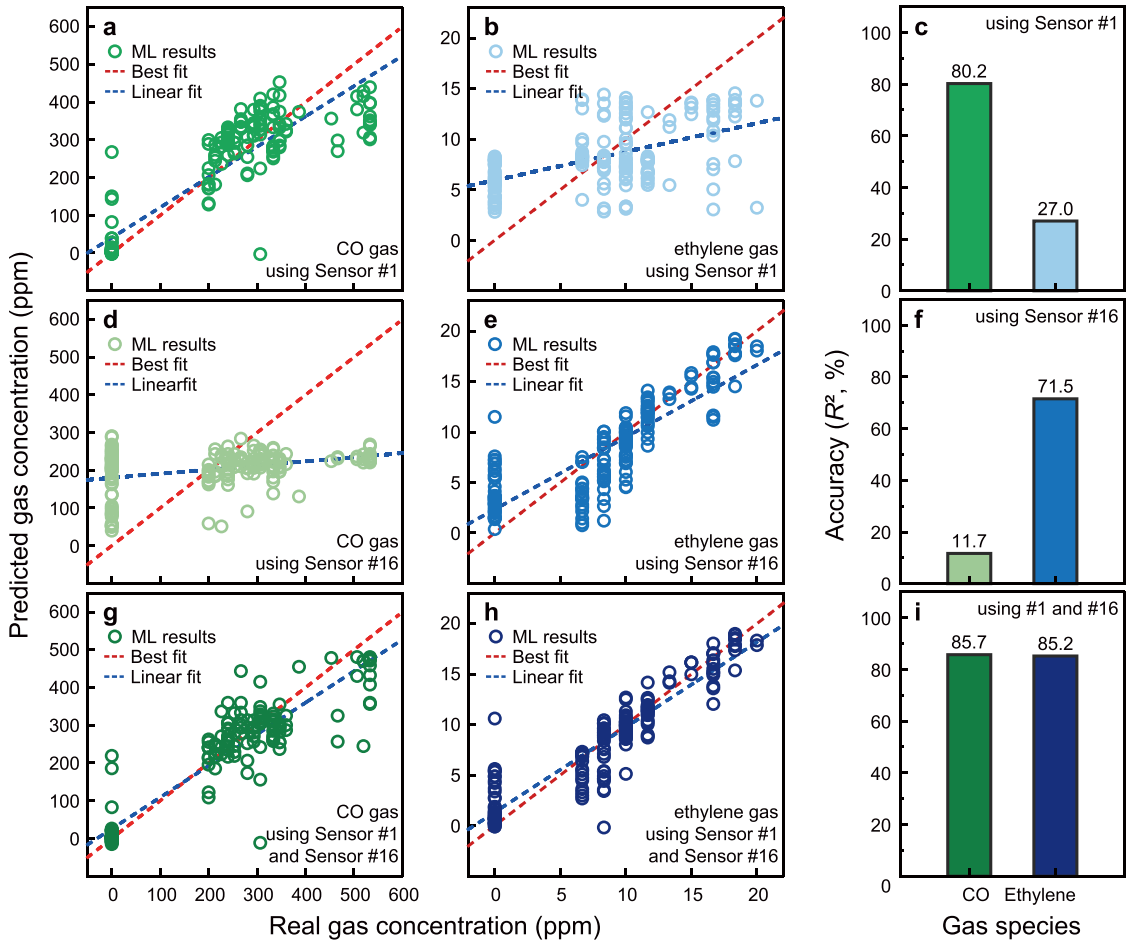

Figure 3. Plot of predicted concentration vs real gas concentration of CO and ethylene using (a,b) sensor #1, (d,e) sensor #16, and (g,h) sensor #1 combined with sensor #16. Accuracy profiles acquired from ML for CO and ethylene gases using (c) sensor #1, (f) sensor #16, and (i) sensor #1 combined with sensor #16.

heater as the sensor platform. The measurement was conducted by the continuous acquisition of the 16-sensor array signals (electrical current) for a duration of about 12 h without interruption while the concentration levels changed randomly. The concentration transitions were set at random times (in the interval of 80−120 s) and to random concentration levels. Response can be converted to resistance (kΩ) by 40.000/R, where R is the value of response.[33] ML was conducted using MATLAB software for conducting the support vector machine (SVM) model with the k-fold validation method. Based on the datasets, the training data was organized for ML, as described in Figure 1. Time-evolution gas response curves for an array containing 16 commercial gas sensors were acquired under exposure to mixture gases (CO + ethylene) with diverse concentrations, as displayed in Figure 1a,b. The dynamic response curve corroborates a gas injection-dependent variation in the time-domain electrical signal, in which the maximized electrical conductivity can be defined as the gas response value. Based on these results, it can be ascertained that the 16-unit sensors exhibited discernible gas responses by altering the concentration of the target gas mixture. To predict the concentration of multiple gases using an ML technique, we adopted the SVM model with k-fold cross-validation (k = 5) in MATLAB software, as represented in Figure 1c. Since two classes of datasets consisting of labeled data (or answer data) and feature data were needed for utilizing the ML method, we rationally assigned the target gas concentrations and gas response as the labeled data and feature data, respectively, as represented in Figure 1d. The details of the experimental conditions are described in the Supporting Information.

To verify the concentration discrimination capability *via* ML for individual gas sensors with differentiated selectivity for CO and ethylene, two representative sensors were prudently selected from the sensor array (sensors #1 and #16). Sensor #1 (TGS 2600, Figaro) possesses high selectivity for gaseous air contaminants such as H_2 and CO, whereas sensor #16 (TGS 2620, Figaro) possesses a high response for ethylene. The selection of two representative sensors enables us to hint at a correlation between the ML-based concentration discrimination capability and discernible gas selectivity. From Figure 2a,b, sensors #1 and #16 show distinct response signals for CO and ethylene gases, and a gas concentration-dependent variation in the response can readily be discerned for each gas. As expected, the response extracted from sensor #1 was more sensitive to altering the concentration of CO (red shaded region), and the response of sensor #16 was more sensitive to ethylene (blue shaded region). The gas response of sensor #1 corresponding to the individual CO (ethylene) gas without the ethylene (CO) gas as a function of the gas concentration is plotted in Figure 2d,e, for a detailed comparison of the selectivity factor for sensor #1. In addition, the concentration-

https://doi.org/10.1021/acsomega.1c02721
ACS Omega 2021, 6, 23155−23162

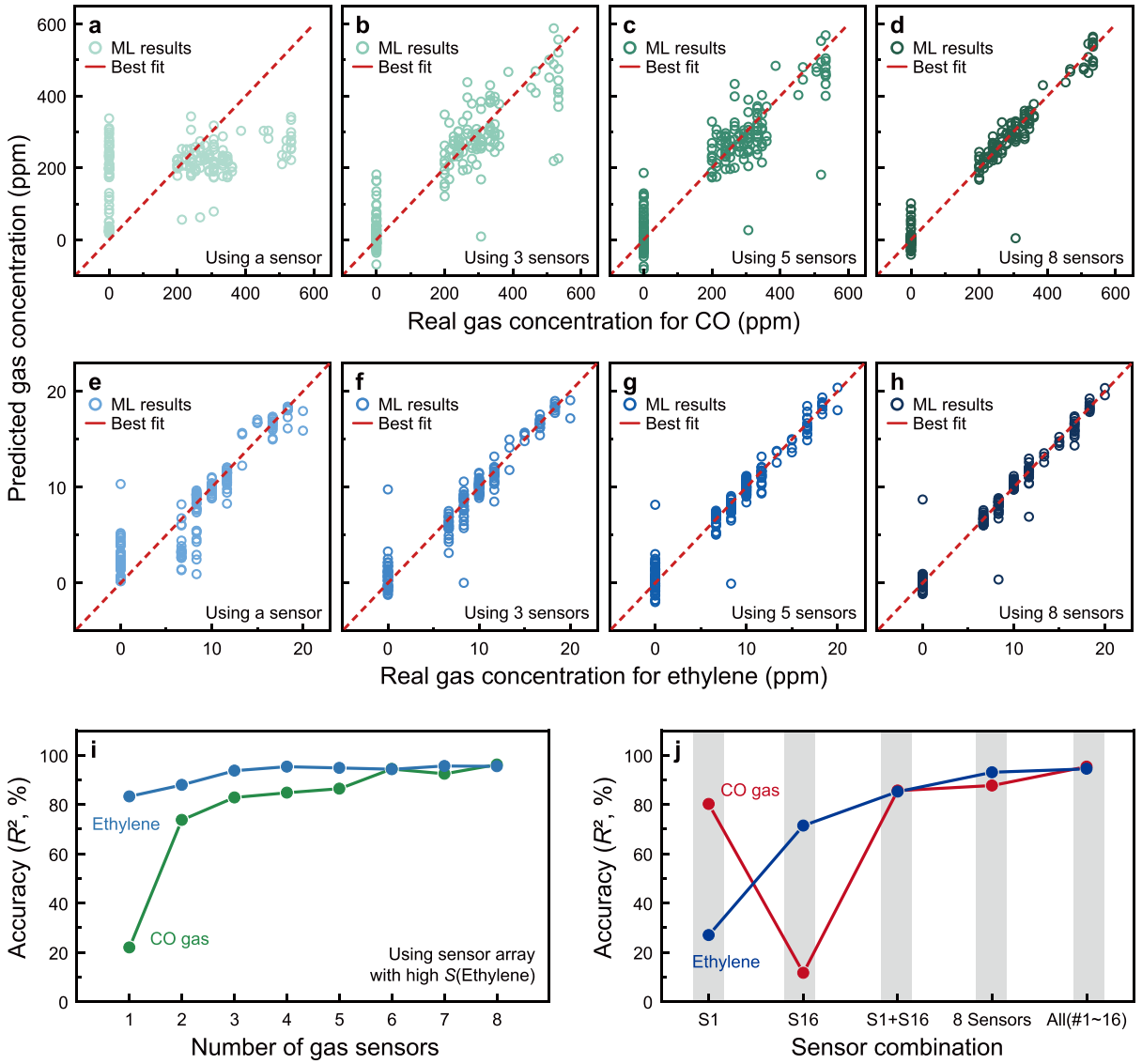

Figure 4. Relationships of predicted gas concentration vs real gas concentration for (a–d) CO and (e–h) ethylene with increasing numbers of unit sensors. Accuracy profiles of the machine learning results with altering (i) number of unit sensors and (j) combination of sensors.

dependent gas response of sensor #1 for ethylene and CO target gases is summarized as a contour plot in Figure 2f. From the results shown in Figure 2d–f, the response gained from sensor #1 was influenced by regulating the concentration of the two gases, in which the concentration of CO gas predominantly affects the gas response of sensor #1, as expressed by $S_1(\mathrm{CO}) > S_1(\mathrm{ethylene})$. An identical analysis was conducted for sensor #16, and the extracted results are summarized in Figure 2g–i. Contrary to sensor #1, sensor #16 showed a higher selectivity factor for ethylene, as denoted by $S_{16}(\mathrm{CO}) < S_{16}(\mathrm{ethylene})$. To investigate the discernable trend of other gas sensors in the array, a repeated analysis was performed on sensors #2 to #15, as summarized in Figure S1, corroborating that the gas sensors with high selectivity factors for CO gas were sensors #1, #9, and #10, and those for ethylene gas corresponded to sensors #3, #4, #7, #8, #11, #12, #15, and #16 ($S_{3,4,7,8,11,12,15}(\mathrm{CO}) < S_{3,4,7,8,11,12,15}(\mathrm{ethylene})$).

The primary goal of this study is to ascertain the correlation between the selectivity factor for a specific gas and the prediction accuracy of each gas concentration in the gas mixture. Accordingly, the data acquired from CO-sensitive sensor #1, ethylene-sensitive sensor #16, and sensor #1 combined with sensor #16 were constructed for ML by using the SVM model with the *k*-fold cross-validation method. The prediction results of CO and ethylene concentrations for sensors #1 and #16 are displayed in Figure 3a–f. The accuracy (R^2) can be calculated using the residual scatter from the fitting line as follows

$$\mathrm{accuracy}(R^2, \%) = 1 - \frac{\sum (y - p)^2}{\sum (y - \bar{y})^2} \tag{3}$$

where y is the real value, p is the predicted value, and $\bar{y}$ is the mean of the real value at the specified corresponding gas concentration. Then, $y - p$ can be described as a residual scatter from the prediction of the real value through the machine learning results. $y - \bar{y}$ is the total variance. In general, because a higher R^2 leads to a well-fitted model compared with the real values, the accuracy of the training model from the SVM model can be estimated using the R^2 value. The residual plots are summarized in Figure S2, and the accuracy results are shown in Figure 3c,f. To clearly observe the scattered values

https://doi.org/10.1021/acsomega.1c02721
ACS Omega 2021, 6, 23155–23162

compared to the best fit (red dashed line), another linear fitting line (blue dashed line) for the scatter was involved in the prediction scatter plots, as shown in Figure 3. The estimated values for the slope and intercept are summarized in Table S1. As we expected, the ML result for sensor #1 exhibits a high scored accuracy of 80.2% for CO gas and a relatively low accuracy of 27.0% for ethylene gas. Conversely, we ascertained that the result from sensor #16 presents an accuracy of 11.7% for CO and 71.5% for ethylene gas. Intriguingly, the concentration discrimination capability *via* ML for both gases was accomplished by the coupling of sensors #1 and #16 (CO of 85.7% and ethylene of 86.2%), as presented in Figure 3g−i. These results can be summarized with a notation of the prediction accuracy as "*A*" and target gas as "X" as follows

$$A_1(\mathrm{CO}) = 80.2\%,\ A_1(\mathrm{ethylene}) = 27.0\% \quad (4)$$

$$A_{16}(\mathrm{CO}) = 11.7\%,\ A_{16}(\mathrm{ethylene}) = 71.5\% \quad (5)$$

$$A_{1+16}(\mathrm{CO}) = 85.7\%,\ A_{1+16}(\mathrm{ethylene}) = 86.7\% \quad (6)$$

These results corroborate a couple of salient phenomena for the predictive capability *via* ML. First, there is a strong correlation between the high selectivity factor of gas sensors and ML results associated with prediction accuracy, which is a proportional relationship

$$S_1(\mathrm{CO}) > S_1(\mathrm{ethylene}) \rightarrow A_1(\mathrm{CO}) > A_1(\mathrm{ethylene}) \quad (7)$$

$$S_{16}(\mathrm{CO}) < S_{16}(\mathrm{ethylene}) \rightarrow A_{16}(\mathrm{CO}) < A_{16}(\mathrm{ethylene}) \quad (8)$$

Second, the enhancement of the prediction accuracy of an elemental sensor with a low sensitivity factor can be attained by a complementary combination of the other sensors with a high selectivity factor.

$$A_1(\mathrm{ethylene}) < A_{1+16}(\mathrm{ethylene}),\ A_{16}(\mathrm{CO}) < A_{1+16}(\mathrm{CO}) \quad (9)$$

Finally, the prediction accuracy can also be boosted by combining the sensor having even a low selectivity factor due to an increase in feature data, $A_1(\mathrm{CO}) < A_{1+16}(\mathrm{CO})$ and $A_{16}(\mathrm{ethylene}) < A_{1+16}(\mathrm{ethylene})$, which hints that a reliable gas recognition system can be accomplished by applying ML to a sensor array system consisting of multiple sensors with a low selectivity factor.

To validate our suggestion, the prediction accuracy of CO and ethylene gas concentrations by altering the number of unit sensors #3, #4, #7, #8, #11, #12, #15, and #16 reveals a nearly identical aspect of ethylene gas (Figure S1) with a relatively low sensitivity factor for CO gas, as shown in Figure 4a−h. The combination of unit sensors corresponds to #3 for one sensor, #3, #4, and #7 for three sensors, #3, #4, #7, #8, and #11 for five sensors, and #3, #4, #7, #8, #11, #12, #15, and #16 for eight sensors. The dependencies of prediction accuracy (R^2) for CO and ethylene gases according to the variation in the number of unit sensors and the combination of unit sensors are summarized in Figure 4i,j, respectively. Their residual plots are also summarized in Figures S3 and S4. It is worth noting that the prediction accuracy for CO concentration is accompanied by an increase in the number of unit sensors (22.1% using a single sensor and 96.3% using eight sensors). The prediction accuracy for the concentration of ethylene gas was also enhanced from 83.3 to 95.5%. Based on our findings, we can conclude that (i) the enhancement of prediction accuracy of an elemental sensor with a low sensitivity factor can be attained by a complementary combination of the other sensor with a high selectivity factor, and further, (ii) it can also be boosted by combining the sensor having even a low selectivity factor due to an increase in feature data. These results can be supported by the improvement in the prediction accuracy of ML owing to the increase in the amount of feature data and also the complementary synergetic effect through the sensor array implementation, as proved in previous studies.[34,35]

CONCLUSIONS

In conclusion, we reported a strategy for the optimal sensor configuration and combination to improve the accuracy of ML-based prediction of gas concentrations using a sensor array system. This strategy permits the minimization of the massive amount of data required for ML and saves efforts to extract the critical features effectively. The most basic feature data of the gas sensor, response, was obtained from the sensor array system composed of 16 sensors, and a dataset was constructed. The correlation between the selectivity factor and prediction accuracy was systemically investigated using the SVM model for ML with the *k*-fold cross-validation protocol. Then, we finally derived the optimal sensor configuration and combination to improve the accuracy of ML-based prediction of concentrations using a sensor array system. It is also envisaged that this methodology will corroborate an adequate solution for prediction and recognition based on ML using a versatile sensor array system.

EXPERIMENTAL SECTION

An open sensor array dataset collected from the University of California Irvine (UCI) was used, which contains the dynamic gas responses gained from arrays of 16 commercial sensors under ethylene and CO mixtures in air with diverse concentrations. The gas sensor array platform was consolidated with a data acquisition system and a flow controlling system. The measurement was conducted by the continuous acquisition of the 16-sensor array signals with a data acquisition board for a duration of about 12 h without interruption while the concentration levels changed randomly. Machine learning (ML) was conducted using MATLAB software for conducting the support vector machine (SVM) model with the *k*-fold validation method. Based on the datasets, the training data was organized for ML. Detailed methods and procedures are described in the Supporting Information.

ASSOCIATED CONTENT

Supporting Information

The Supporting Information is available free of charge at https://pubs.acs.org/doi/10.1021/acsomega.1c02721.

Analysis of gas responses of different CO and ethylene gas concentrations for all sensors and a plot of residual scatter from prediction values by machine learning for CO and ethylene gas concentrations using different datasets (PDF)

AUTHOR INFORMATION

Corresponding Authors

Wooseok Song − *Thin Film Materials Research Center, Korea Research Institute of Chemical Technology (KRICT), Daejeon 34114, Republic of Korea;* orcid.org/0000-0002-

https://doi.org/10.1021/acsomega.1c02721
ACS Omega 2021, 6, 23155−23162

0487-2055; Phone: +82-42-860-7295; Email: wssong@krict.re.kr

Ki-Seok An − *Thin Film Materials Research Center, Korea Research Institute of Chemical Technology (KRICT), Daejeon 34114, Republic of Korea;* orcid.org/0000-0001-8250-7347; Phone: +82-42-860-7356; Email: ksan@krict.re.kr

Authors

Garam Bae − *Thin Film Materials Research Center, Korea Research Institute of Chemical Technology (KRICT), Daejeon 34114, Republic of Korea*

Minji Kim − *Thin Film Materials Research Center, Korea Research Institute of Chemical Technology (KRICT), Daejeon 34114, Republic of Korea*

Sung Myung − *Thin Film Materials Research Center, Korea Research Institute of Chemical Technology (KRICT), Daejeon 34114, Republic of Korea;* orcid.org/0000-0003-2030-2391

Sun Sook Lee − *Thin Film Materials Research Center, Korea Research Institute of Chemical Technology (KRICT), Daejeon 34114, Republic of Korea;* orcid.org/0000-0002-3518-5952

Complete contact information is available at: https://pubs.acs.org/10.1021/acsomega.1c02721

Author Contributions

The manuscript was written through contributions of all authors. All authors have given approval to the final version of the manuscript.

Notes

The authors declare no competing financial interest.

■ ACKNOWLEDGMENTS

This research was supported by the Multi-Ministry Collaborative R&D Program through the National Research Foundation of Korea (NRF) funded by KNPA, MSIT, MOTIE, ME, and NFA (NRF-2017M3D9A1073858 and NRF-2017M3D9A1073502) and a grant from the Advanced Technology Center (ATC) Program (10077265) funded by the Ministry of Trade, Industry & Energy of the Republic of Korea.

■ REFERENCES

(1) Deshmukh, K.; Kovářík, T.; Khadheer Pasha, S. K.; Khadheer Pasha, S. K. State of the Art Recent Progress in Two Dimensional MXenes Based Gas Sensors and Biosensors: A Comprehensive Review. *Coord. Chem. Rev.* **2020**, *424*, 213514.

(2) Singh, E.; Meyyappan, M.; Nalwa, H. S. Flexible Graphene-Based Wearable Gas and Chemical Sensors. *ACS Appl. Mater. Interfaces* **2017**, *9*, 34544−34586.

(3) Yavari, F.; Koratkar, N. Graphene-Based Chemical Sensors. *J. Phys. Chem. Lett.* **2012**, *3*, 1746−1753.

(4) Alzate-Carvajal, N.; Luican-Mayer, A. Functionalized Graphene Surfaces for Selective Gas Sensing. *ACS Omega* **2020**, *5*, 21320−21329.

(5) Shaffer, R. E.; Rose-Pehrsson, S. L.; McGill, R. A. A Comparison Study of Chemical Sensor Array Pattern Recognition Algorithms. *Anal. Chim. Acta* **1999**, *384*, 305−317.

(6) Nicolas, J.; Romain, A. C.; Wiertz, V.; Maternova, J.; André, P. Using the Classification Model of an Electronic Nose to Assign Unknown Malodours to Environmental Sources and to Monitor Them Continuously. *Sens. Actuators, B Chem.* **2000**, *69*, 366−371.

(7) Stetter, J. R.; Findlay, M. W., Jr.; Schroeder, K. M.; Yue, C.; Penrose, W. R. Quality Classification of Grain Using a Sensor Array and Pattern Recognition. *Anal. Chim. Acta* **1993**, *284*, 1−11.

(8) Kwon, H.; Yoon, J.-S.; Lee, Y.; Kim, D. Y.; Baek, C.-K.; Kim, J. K. An Array of Metal Oxides Nanoscale Hetero P-n Junctions toward Designable and Highly-Selective Gas Sensors. *Sens. Actuators, B* **2018**, *255*, 1663−1670.

(9) Zheng, W.; Xu, Y.; Zheng, L.; Yang, C.; Pinna, N.; Liu, X.; Zhang, J. MoS_2 Van Der Waals p−n Junctions Enabling Highly Selective Room-Temperature NO_2 Sensor. *Adv. Funct. Mater.* **2020**, *30*, 2000435.

(10) Jiang, P.; Zhang, H.; Chen, C.; Liang, J.; Luo, Y.; Zhang, M.; Cai, M. Co_3O_4−SnO_2 Nanobox Sensor with a PN Junction and Semiconductor−Conductor Transformation for High Selectivity and Sensitivity Detection of H 2 S. *CrystEngComm* **2017**, *19*, 5742−5748.

(11) Tabata, H.; Sato, Y.; Oi, K.; Kubo, O.; Katayama, M. Bias- and Gate-Tunable Gas Sensor Response Originating from Modulation in the Schottky Barrier Height of a Graphene/MoS_2 van Der Waals Heterojunction. *ACS Appl. Mater. Interfaces* **2018**, *10*, 38387−38393.

(12) Singh, A.; Uddin, M. A.; Sudarshan, T.; Koley, G. Tunable Reverse-Biased Graphene/Silicon Heterojunction Schottky Diode Sensor. *Small* **2014**, *10*, 1555−1565.

(13) Zhou, T.; Sang, Y.; Wang, X.; Wu, C.; Zeng, D.; Xie, C. Pore Size Dependent Gas-Sensing Selectivity Based on ZnO@ZIF Nanorod Arrays. *Sens. Actuators, B* **2018**, *258*, 1099−1106.

(14) Tian, H.; Fan, H.; Li, M.; Ma, L. Zeolitic Imidazolate Framework Coated ZnO Nanorods as Molecular Sieving to Improve Selectivity of Formaldehyde Gas Sensor. *ACS Sensors* **2016**, *1*, 243−250.

(15) Jeon, I. S.; Bae, G.; Jang, M.; Song, W.; Myung, S.; Lee, S. S.; Jung, H.-K.; Hwang, J.; An, K.-S. A Synergistic Combination of Zinc Oxide Nanowires Array with Dual-Functional Zeolitic Imidazolate Framework-8 for Hybrid Nanomaterials-Based Gas Sensors. *Compos. Part B Eng.* **2020**, *180*, 107552.

(16) Betts, T. A.; Tipple, C. A.; Sepaniak, M. J.; Datskos, P. G. Selectivity of Chemical Sensors Based on Micro-Cantilevers Coated with Thin Polymer Films. *Anal. Chim. Acta* **2000**, *422*, 89−99.

(17) Jang, M.; Lee, J.; Park, S. Y.; Lee, J.; Lee, K. M.; Song, W.; Myung, S.; Lee, S. S.; Jung, H.-K.; Kang, Y. C.; Kwak, S. K.; An, K.-S. Rational Surface Modification of ZnO with Siloxane Polymers for Room-Temperature-Operated Thin-Film Transistor-Based Gas Sensors. *Appl. Surf. Sci.* **2021**, *542*, 148704.

(18) Yang, D.-J.; Kamienchick, I.; Youn, D. Y.; Rothschild, A.; Kim, I.-D. Ultrasensitive and Highly Selective Gas Sensors Based on Electrospun SnO_2 Nanofibers Modified by Pd Loading. *Adv. Funct. Mater.* **2010**, *20*, 4258−4264.

(19) Suematsu, K.; Watanabe, K.; Tou, A.; Sun, Y.; Shimanoe, K. Ultraselective Toluene-Gas Sensor: Nanosized Gold Loaded on Zinc Oxide Nanoparticles. *Anal. Chem.* **2018**, *90*, 1959−1966.

(20) Schroeder, V.; Evans, E. D.; Wu, Y.-C. M.; Voll, C.-C. A.; McDonald, B. R.; Savagatrup, S.; Swager, T. M. Chemiresistive Sensor Array and Machine Learning Classification of Food. *ACS Sensors* **2019**, *4*, 2101−2108.

(21) Tonezzer, M. Selective Gas Sensor Based on One Single SnO_2 Nanowire. *Sens. Actuators, B* **2019**, *288*, 53−59.

(22) Khalid, S.; Khalil, T.; Nasreen, S. A Survey of Feature Selection and Feature Extraction Techniques in Machine Learning. In *2014 Science and Information Conference*; IEEE, 2014; pp. 372−378. doi: DOI: 10.1109/SAI.2014.6918213.

(23) Rodrigues, D.; Papa, J. P.; Adeli, H. Meta-Heuristic Multi- and Many-Objective Optimization Techniques for Solution of Machine Learning Problems. *Expert Syst.* **2017**, *34*, No. e12255.

(24) Tong, M. M.; Yu, Z.; Mei-Xing. The mixed inflammable gas analysis based on BP neural network. *Acta Metrologica Sinica* **2006**, *2*, 169.

(25) Dragonieri, S.; Schot, R.; Mertens, B.; Cessie, S. An electronic nose in the discrimination of patients with Asthma and Controls. *J. Allergy Clin. Immunol.* **2007**, *120*, 856−862.

(26) Peng, P.; Zhao, X.; Pan, X.; Ye, W. Gas classification using deep convolutional neural networks. *Sensors* **2018**, *18*, 157.
(27) Cortes, C.; Vapnik, V. Support-Vector Networks. *Mach. Learn.* **1995**, *20*, 273−297.
(28) Maxwell, A. E.; Warner, T. A.; Fang, F. Implementation of Machine-Learning Classification in Remote Sensing: An Applied Review. *Int. J. Remote Sens.* **2018**, *39*, 2784−2817.
(29) Kotsiantis, S. B.; Zaharakis, I.; Pintelas, P. Supervised Machine Learning: A Review of Classification Techniques. *Emerg. Artif. Intell. Appl. Comput. Eng.* **2007**, *160*, 3−24.
(30) Han, L.; Zhou, W.; Xiang, C. High-Rate Electrochemical Reduction of Carbon Monoxide to Ethylene Using Cu-Nanoparticle-Based Gas Diffusion Electrodes. *ACS Energy Lett.* **2018**, *3*, 855−860.
(31) Jeong, S.-Y.; Moon, Y. K.; Kim, T.-H.; Park, S.-W.; Kim, K. B.; Kang, Y. C.; Lee, J.-H. A New Strategy for Detecting Plant Hormone Ethylene Using Oxide Semiconductor Chemiresistors: Exceptional Gas Selectivity and Response Tailored by Nanoscale Cr_2O_3 Catalytic Overlayer. *Adv. Sci.* **2020**, *7*, 1903093.
(32) Chen, R.; Su, H.-Y.; Liu, D.; Huang, R.; Meng, X.; Cui, X.; Tian, Z.-Q.; Zhang, D. H.; Deng, D. Highly Selective Production of Ethylene by the Electroreduction of Carbon Monoxide. *Am. Ethnol.* **2020**, *132*, 160−166.
(33) Fonollosa, J.; Sheik, S.; Huerta, R.; Marco, S. Reservoir Computing Compensates Slow Response of Chemosensor Arrays Exposed to Fast Varying Gas Concentrations in Continuous Monitoring. *Sens. Actuators B Chem.* **2015**, *215*, 618−629.
(34) Al-Jarrah, O. Y.; Yoo, P. D.; Muhaidat, S.; Karagiannidis, G. K.; Taha, K. Efficient Machine Learning for Big Data: A Review. *Big Data Res.* **2015**, *2*, 87−93.
(35) Stockwell, D. R. B.; Peterson, A. T. Effects of Sample Size on Accuracy of Species Distribution Models. *Ecol. Modell.* **2002**, *148*, 1−13.

https://doi.org/10.1021/acsomega.1c02721
ACS Omega 2021, 6, 23155−23162